

TALAT Lecture 3701

Formability Characteristics of Aluminium Sheet

29 pages, 30 figures

Advanced Level

prepared by
K. Siegert and S. Wagner, Institut für Umformtechnik, Universität Stuttgart

Objectives:

- to describe the fundamental formability characteristics of automotive aluminium sheet metals
- to learn about the various methods to characterize the forming behaviour and the forming limits

Prerequisites:

- general background in production engineering and sheet metal forming

Date of Issue: 1994

© EAA-European Aluminium Association

3701 Formability Characteristics of Aluminium Sheet

Table of Contents

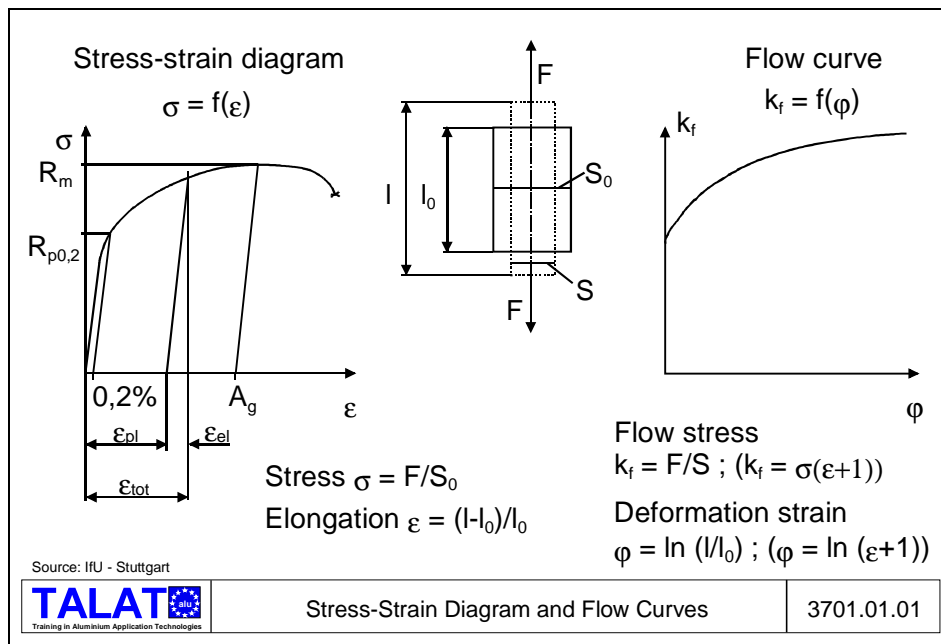
3701 Formability Characteristics of Aluminium Sheet	2
3701.01 Uniaxial Tensile Tests	3
Preparing Tensile Specimens from a Sheet.....	5
Stress-Strain Curves of Aluminium Sheet Alloys	6
Flow Curves of Aluminium Alloys.....	7
Definition of the Strain-Hardening Exponent n	8
Anisotropy.....	9
Definition of Anisotropic Values.....	11
Anisotropy as a Function of Rolling Direction.....	11
Representation of the Vertical Anisotropy Using Polar Coordinates	12
3701.02 Aluminium Alloys	13
Fields of Application of Aluminium Body Sheet Alloys.....	14
Compositions and Properties of Aluminium Car Body Sheet Alloys.....	14
3701.03 Technological Testing Methods	14
Hydraulic Bulge Test	16
Plotted Flow Curves for a Heat-Treatable Aluminium Alloy.....	18
Erichsen Cupping Test.....	18
Cup Drawing Test according to Swift.....	20
Effect of the Blank Diameter to Thickness Ratio on Limiting Draw Ratio.....	22
Drawability of Materials according to Engelhardt.....	23
Creating the Forming Limit Diagram (FLD)	24
3701.04 List of Figures	29

The experimental results shown here are exemplary and qualitative. They are not absolutely representative for the given material. The material properties have a range of scatter which depends on the supplier and the charge.

The following results shall, on the other hand, clearly define which information regarding the materials can be obtained from the individual tests.

3701.01 Uniaxial Tensile Tests

The uniaxial tensile test is the basis for defining mechanical properties of materials. It is standardised in DIN EN 10 002 for specimens with round or rectangular cross sections. **Figure 3701.01.01** defines the terms of the stress-strain diagram and flow curve obtained from the uniaxial tensile test.



An evaluation of the results of the test according to DIN EN 10 002 for setting up a flow curve is only possible up to the uniform elongation A_g . The big advantage of the tensile test is that the strain and the tensile force can be easily and simply converted to a degree of deformation and flow stress without using any flow criteria. Besides, this process is not affected by any frictional effects. The main disadvantage of the tensile test is that at relatively small degrees of deformation, a local necking sets in. For a uniaxial tensile stress condition, the maximum degree of deformation which can be attained is given by

$$\varphi_{gl} = \ln(1 + A_g) < 0.3$$

The tensile test delivers the stress-strain diagram, from which the characteristic values are determined and used as a basis for strength calculations. The measured tensile force F is based on the original cross-sectional area S_0 of the specimen. Since, however, the cross-sectional area changes continuously during the test, the true stresses are not determined.

$$\sigma = F/S_0$$

For determining the instantaneous elongation, the change in length dL is referred to the original length L_0 :

$$d\varepsilon = dL/L_0$$

The degree of deformation. i.e. the strain ε can be calculated by integration:

$$\varepsilon = \int_{L_0}^{L_1} dL / L_0 = (L_1 - L_0) / L_0$$

In the region of uniform elongation, the flow curve can be calculated quite easily from the force-elongation curve (or stress-strain curve). The positive slope of the tensile force (stress) curve indicates that in this region the effect of work hardening (strain hardening) of the material is more pronounced than the effect of the reduction in area (cross-section). A uniaxial (one-dimensional) state of stress exists in this region of the curve and the stress is distributed uniformly throughout the specimen.

When the loading of the specimen is increased further, a peak value is attained in the force-elongation curve. A further increase in deformation is associated with a negative slope of the curve, indicating that the increase of material strength due to work hardening is less than the weakening due to the reduction in area of the specimen. This means that from the peak value onwards, necking starts to occur in the tensile specimen (plastic instability). The evaluation of the tensile test according to DIN EN 10 002 is limited to the region of uniform elongation.

The region extending from the value of maximum force up to rupture of the specimen is characterised by a three-dimensional state of stress accompanied by a non-homogeneous distribution of stress and deformation (strain) across the specimen cross-section. The transverse stresses thus created in the necked zone are the result of deformation restraint of the less elongated transitional regions and of non-axial forces resulting from the deviation of the force flow lines. Further deformation of the sample is limited to the necked region and accompanied by a rapid increase in local deformation rate at that region.

These conditions must be considered and the experimental results correspondingly corrected when determining the flow curve which, according to definition, is measured for a uniaxial state of stress and for a constant deformation rate.

The flow stress, k_f , depends on material, temperature T , degree of deformation φ and deformation rate $\dot{\varphi}$. It is defined for a uniaxial state of stress and a deformation which is as homogeneous as possible:

$$k_f = f(\varphi, \dot{\varphi}, T, \text{material})$$

In order to initiate or to maintain a plastic flow of material, the active stresses actually occurring must exceed a certain characteristic value. In order to determine the material characteristic values in forming technology, it is therefore usual to refer the force (F) to the actual surface area (S).

The stress $k_f = F/S$ is referred to as the flow stress in the region of plastic flow. In order to illustrate the flow curve, this value is graphically depicted as a function of the degree of deformation ϕ .

The uniaxial tensile test is used as an example to explain the definition of degree of deformation. If the change of length, dL is based on the momentary length L , then:

$$d\phi = dL/L$$

The degree of deformation is obtained by integrating this equation over the deformation path :

$$\phi = \int_{L_0}^{L_1} dL / L = \ln(L_1 / L_0)$$

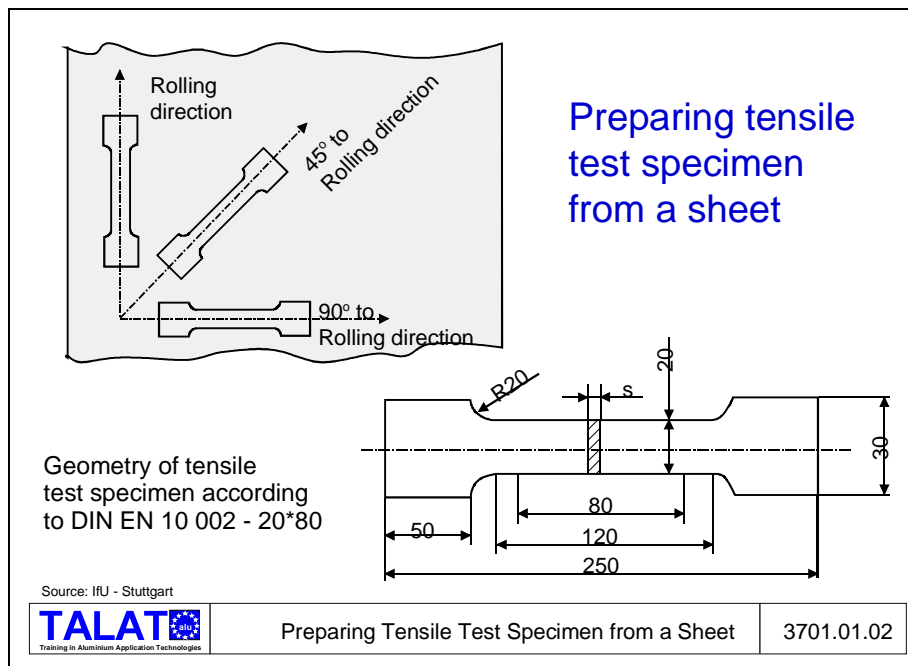
The flow curve can be determined easily from the stress-strain curve, since a correlation exists between the stress, σ , and the flow stress, k_f , or between the strain ϵ and the degree of deformation ϕ .

$$k_f = \sigma (1 + \epsilon/100)$$

$$\phi = \ln (1 + \epsilon/100)$$

Preparing Tensile Specimens from a Sheet

Figure 3701.01.02 shows how tensile specimens are made from sheets and the specimen geometry used.



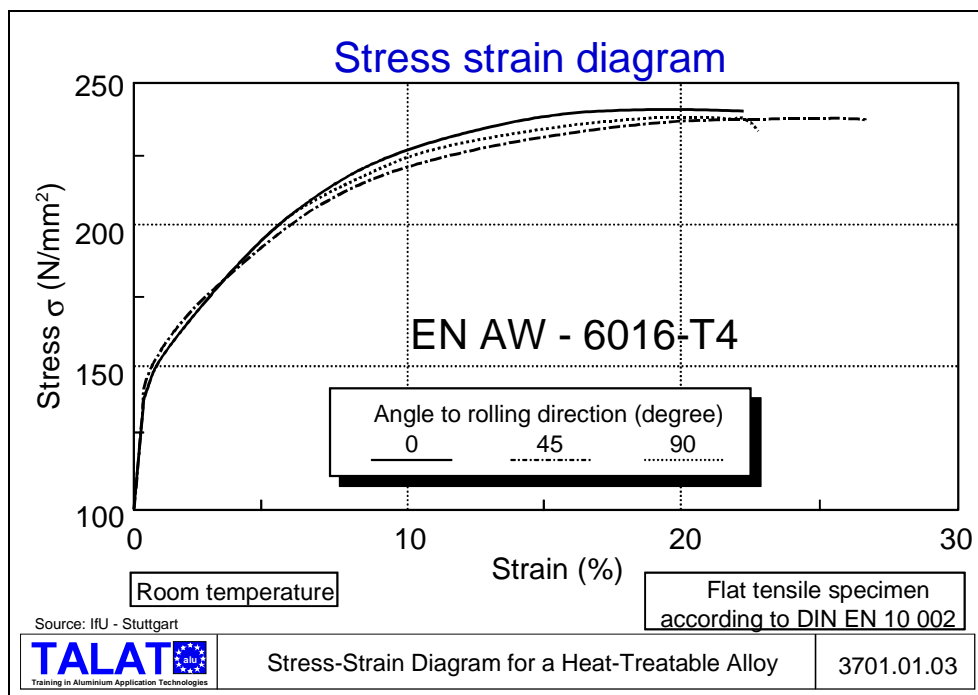
For conducting tensile tests on sheets, non-proportional flat specimens with heads according to DIN EN 10 002 - 20*80 (large ISO flat specimens with a starting length of

$L_0 = 80 \text{ mm}$ and a width of $b_0 = 20 \text{ mm}$) are prepared from the sheet. Tensile specimens are prepared from the sheet metal at 0° , 45° and at 90° to the rolling direction. The tests are conducted at room temperature in a tensile testing machine. During the tensile testing, the tensile force, the elongation of the specimen and the transverse contraction of the specimen are recorded.

From the stress-strain curves, one can obtain the following characteristic values: modulus of elasticity E , either the higher (R_{eH}) and lower (R_{eL}) yield points or the yield strength $R_{p0,2}$, ultimate tensile strength R_m , uniform elongation A_g , total strain to fracture A_{80mm} and information about the normal anisotropy r .

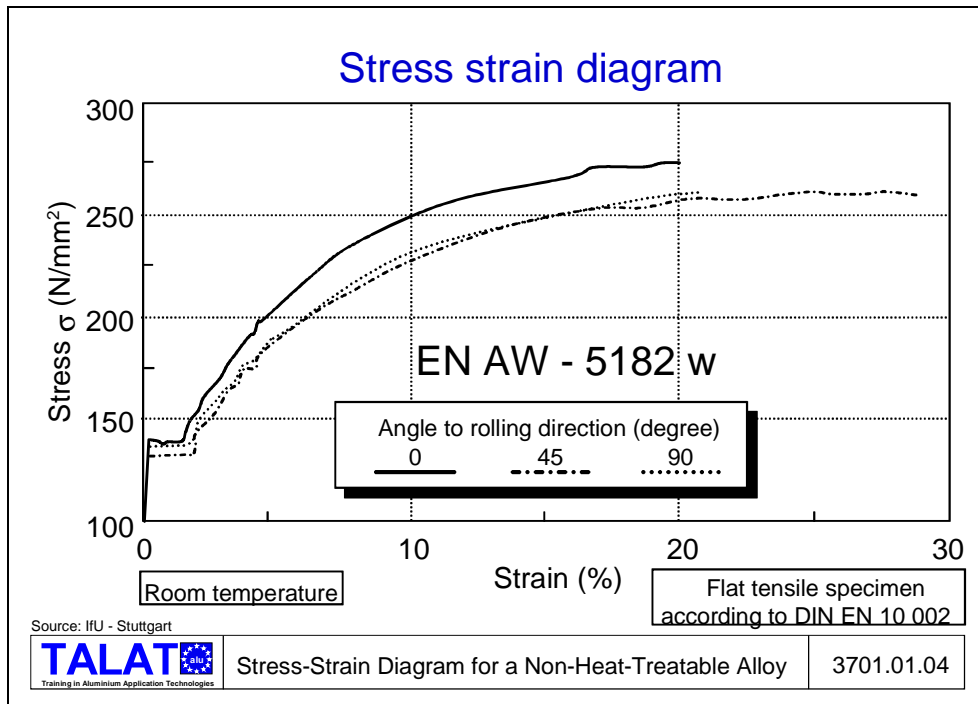
Stress-Strain Curves of Aluminium Sheet Alloys

Most sheet materials exhibit a pronounced influence of the rolling direction on the characteristic property values.



The stress-strain curves in **Figure 3701.01.03** are shown for the naturally aged alloy AlMg0.4Si1.2-T4 tested under 0° , 45° and 90° to the rolling direction. There are marked differences regarding both the maximum stress as well as the maximum elongation that can be obtained.

The non-heat-treatable alloy AlMg5Mn-O shows a similar behaviour, see **Figure 3701.01.04**. As is characteristic for Magnesium-containing aluminium alloys, yield points (upper R_{eH} and lower R_{eL}) and Lüder bands can be discerned up to a strain of approximately 2 %. With further stretching of the specimen deviations from the smooth stress-strain curve indicate the formation of stretcher lines.



Flow Curves of Aluminium Alloys

The flow curves in **Figure 3701.01.05** and **Figure 3701.01.06** depicted for the range of uniform elongation have been calculated from the stress-strain curves shown in **Figure 3701.01.03** and **Figure 3701.01.04** for the alloys AlMg0.4Si1.2-T4 and AlMg5Mn-0, respectively.

Flow curves for unalloyed and low-alloy steels as well as for some non-ferrous metals (e.g., aluminium and its alloys) can very often be calculated from the Ludwik-Hollomon equation:

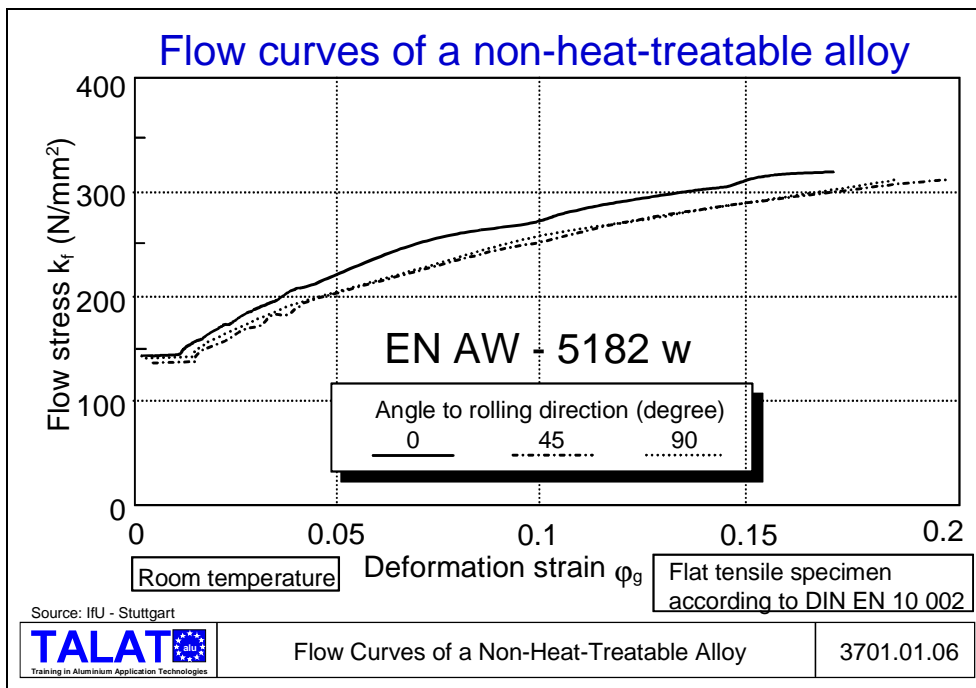
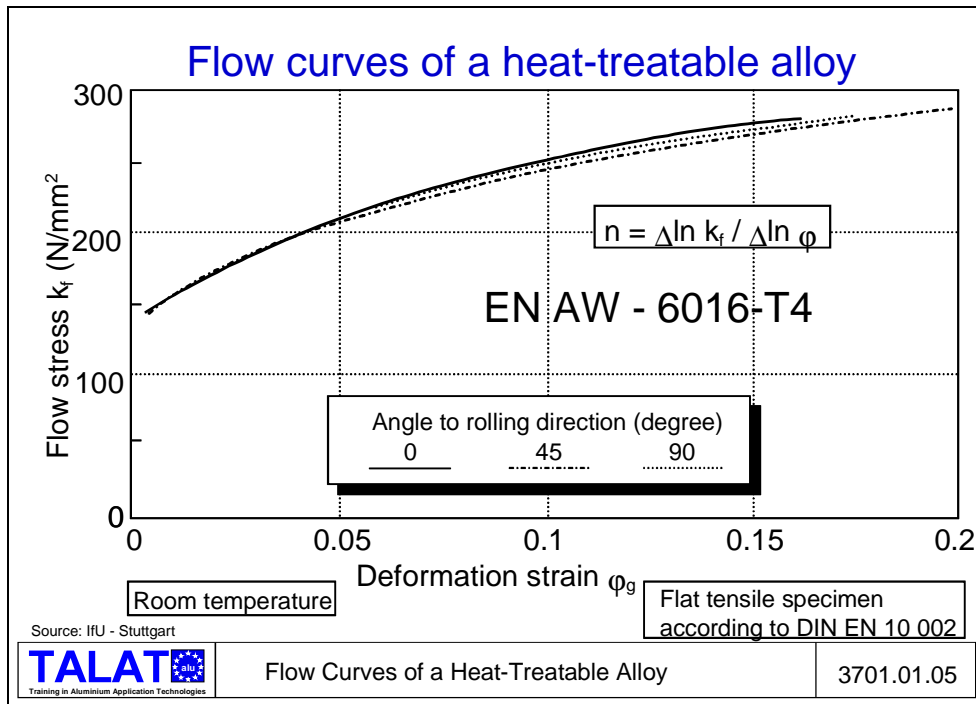
$$k_f = C \varphi^n$$

where C is a constant and n the strain-hardening exponent. This equation is not valid for high-alloy steels and copper, which have a different strain-hardening behaviour.

Using a calculation based on linear regression of the logarithmic flow curve according to Ludwik-Hollomon,

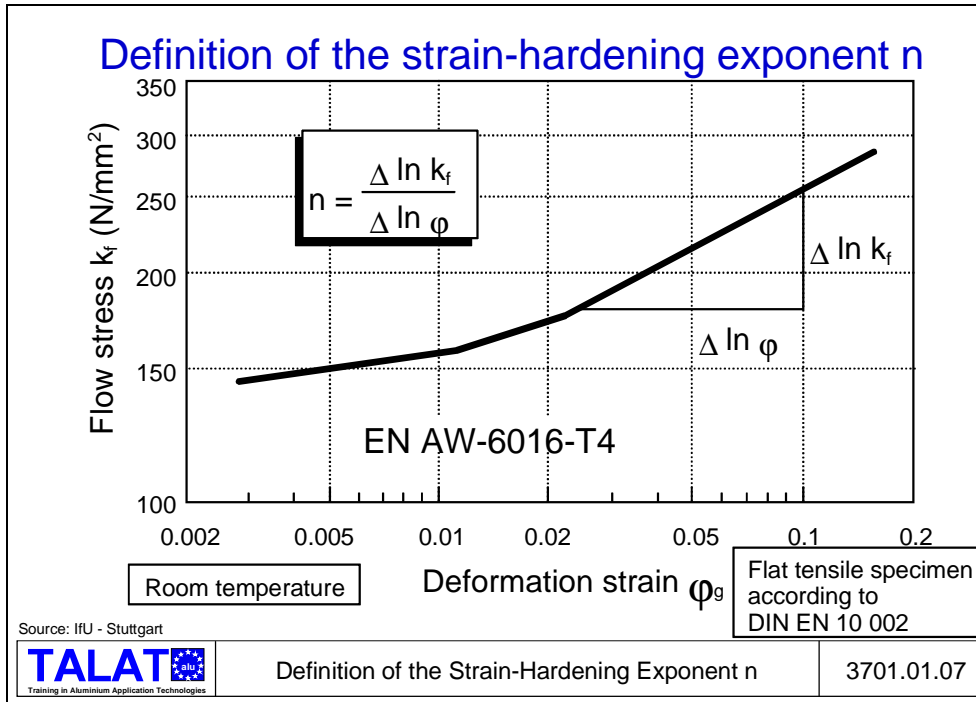
$$\ln k_f = \ln C + n \ln \varphi$$

the values for the strain-hardening exponent n and the constant C can be calculated for the tested material in a region of elongation which must inevitably be stated, e.g. $\varepsilon = 1\% A_g$ (uniform strain) (see also Stahl-Eisen-Prüfblatt 1123).



Definition of the Strain-Hardening Exponent n

As shown in **Figure 3701.01.07**, the flow curve for alloy AlMg0.4Si1.2-T4 is approximately a straight line in a double-logarithmic plot for plastic strains greater than approximately 3 % ($\varphi > 0.02$), which then conforms very well with the Ludwik-Hollomon equation. The strain-hardening exponent n is equal to the slope of the straight line.



The strain-hardening exponent n can be considered to be a measure of the maximum attainable deformation during cold forming.

Stretch forming: The higher the value of n and, consequently, the higher the uniform strain, the lower is the tendency of the material to neck locally. Higher forming forces can be applied to the center regions of the sheet, so that forming of these middle regions can be increased.

Deep drawing: During deep drawing, the limiting draw ratio increases slightly with increasing n -value, since a combined stretch forming/deep drawing action exists at the beginning of the drawing process.

In order to estimate the strain-hardening behaviour, the strain-hardening coefficient can, according to Reihle, be assumed to be equal to the uniform strain

$$n \approx \phi_{gl}$$

During tensile testing the tensile force F , the elongation l of the specimen and the transverse contraction (i.e., the change in the specimen width b) of the specimen are measured, see **Figure 3701.01.08**. From these values and using the law of volume constancy, it is possible to calculate the change in the sheet thickness s .

Anisotropy

Sheets do not have the same properties in all directions. This variation of material properties in relation to the rolling direction is called anisotropy. The reasons for this behaviour of directional dependency of mechanical properties are:

- the anisotropy of crystals (the variation of the properties of the elementary cells with direction)
- the texture (preferred orientation of certain crystallographic planes and directions)
- the grain anisotropy (preferred orientation of grains and grain boundaries, e.g. elongation of grains in the direction of rolling).

The grain anisotropy is mainly the result of the previous cold working process, e.g. cold rolling. The anisotropy plays a very important role during forming processes.

Schematic Illustration of a Flat Tensile Specimen

F ... Tensile force s ... Specimen thickness
 b ... Specimen width l ... Reference length

Source: IfU - Stuttgart

TALAT <small>Training in Aluminium Application Technologies</small>	Schematic Illustration of a Flat Tensile Specimen	3701.01.08
---	---	------------

Definition of Anisotropy Values

Vertical anisotropy:

$$r = \varphi_v / \varphi_s = \ln(b/b_0) / \ln(s/s_0)$$

Average vertical anisotropy:

$$r_m = (r_0 + 2r_{45} + r_{90}) / 4$$

Plane anisotropy:

$$\Delta r = (r_0 - 2r_{45} + r_{90}) / 2$$

better:

$$\Delta r = r_{\max} - r_{\min}$$

Source: IfU - Stuttgart

TALAT <small>Training in Aluminium Application Technologies</small>	Definition of Anisotropy Values	3701.01.09
---	---------------------------------	------------

Definition of Anisotropic Values

A number of characteristic values are used as a measure of anisotropy. For sheet forming, the following characteristic values are important (s. **Figure 3701.01.09**):

The vertical anisotropy r is the ratio of the logarithmic change in sheet width φ_b (true width strain) to the logarithmic change in the sheet thickness φ_s (true thickness strain).

$$r = \varphi_b / \varphi_s = \ln(b/b_0) / \ln(s/s_0)$$

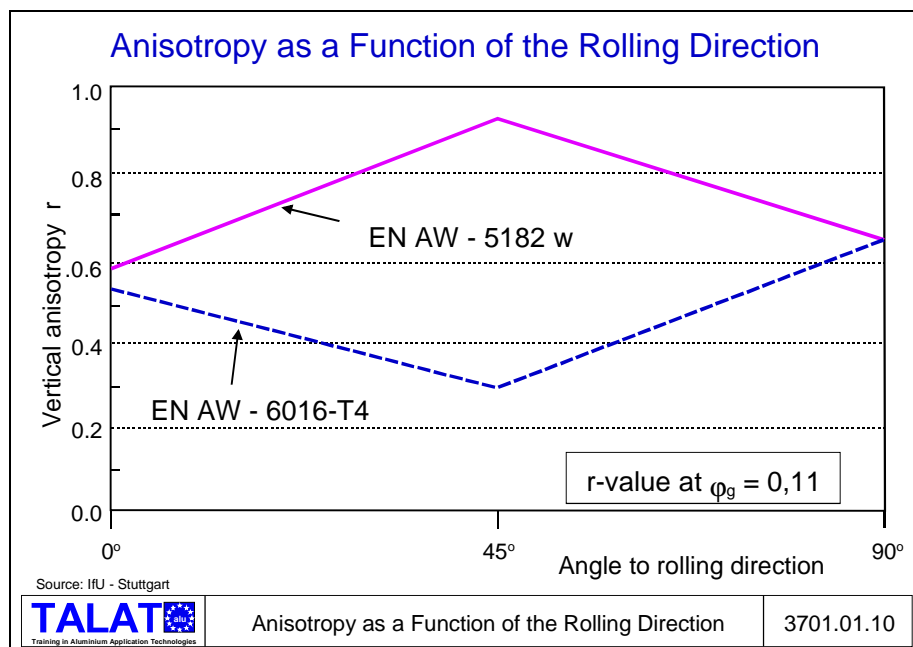
Isotropic materials have a value of $r = 1$.

Materials which have a vertical anisotropic value of $r > 1$, possess a high resistance to plastic flow in the direction of the sheet thickness.

Anisotropy as a Function of Rolling Direction

The value of the vertical anisotropy r is not constant in a sheet plane, but depends on the angle to the rolling direction.

The vertical anisotropy values r as determined by tensile testing are, depending on the material (alloy composition) and the previous treatment, either lowest (e.g., AlMg0.4Si1.2-T4) or highest (e.g., AlMg5Mn-O) at 45° to the rolling direction. This dependency from the rolling direction can be seen clearly in **Figure 3701.01.10** which illustrates values for vertical anisotropy for both aluminium alloys at a deformation strain of $\varphi_g = 0.11$.



From the r values determined at a definite angle to the rolling direction, the average vertical anisotropy r_m can be calculated:

$$r_m = (r_0 + 2r_{45} + r_{90})/4$$

Representation of the Vertical Anisotropy Using Polar Coordinates

A significant measure for the variance of the vertical anisotropy over the sheet plane is the plane anisotropy Δr .

$$\Delta r = (r_0 - 2r_{45} + r_{90})/2$$

For some materials, the following equation is valid:

$$r_{45} \approx (r_0 + r_{90})/2$$

From the above equation one obtains $\Delta r \approx 0$, even though the material is strongly anisotropic. Consequently, it seems to be logical to define the plane anisotropy as

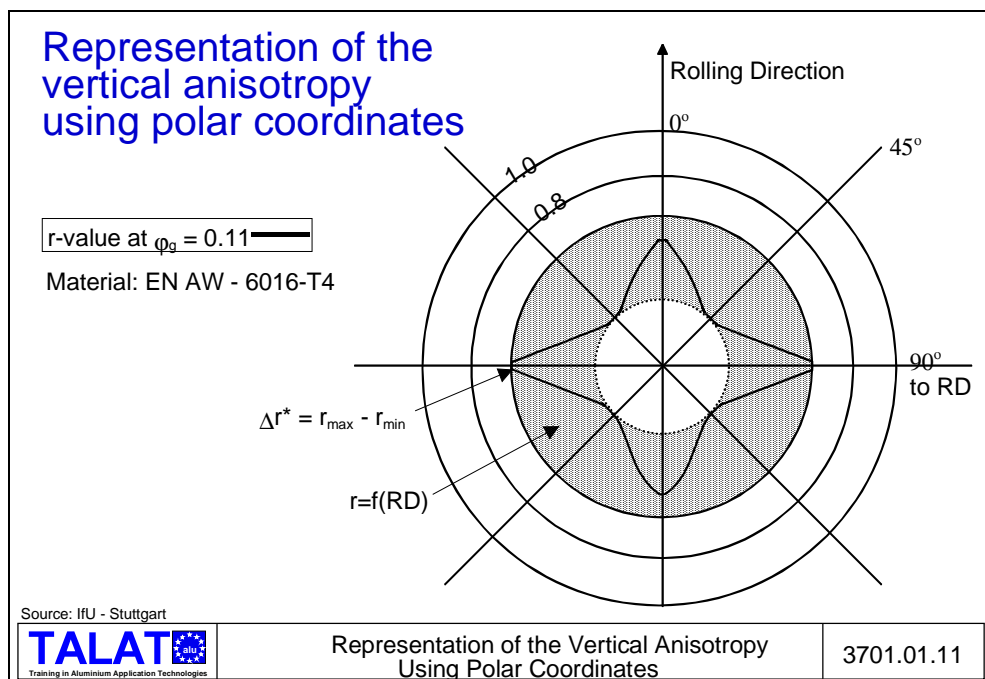
$$\Delta r^* = r_{max} - r_{min}$$

In **Figure 3701.01.11** this Δr^* is depicted as the shaded ring area.

The vertical anisotropy has the following effects during deep drawing:

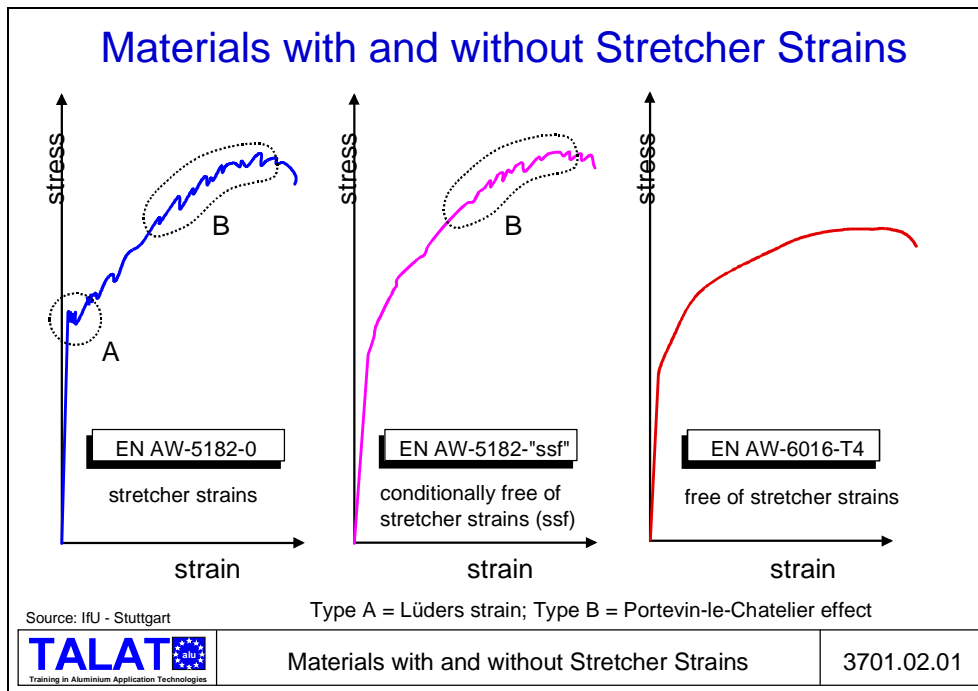
- Small values of r result in a small limiting draw ratio β_{0max} .
- Large values of r result in a large limiting draw ratio β_{0max} .
- The plane anisotropy leads to undesirable earing during the deep drawing of axially symmetrical cups, i.e., the cup height is no longer constant. Earing is expected in those directions for which the largest r values exist. Earing occurs in the 0° and 90° directions for positive Δr values ($\Delta r > 0$). For negative values of Δr ($\Delta r < 0$), earing occurs at 45° to the rolling direction.

As a general rule for deep drawing, the lowest r value (r_{min}) indicates the position in the plane of the sheet with the highest probability of necking. r_{min} is, therefore, preferred to be as high as possible.



3701.02 Aluminium Alloys

The occurrence of stretcher strains during deformation depends very much on the type of aluminium alloy, see **Figure 3701.02.01**. Especially the addition of magnesium in non-age-hardening aluminium alloys renders these alloys prone to yield point phenomena and stretcher strains.



For sheet materials having pronounced yield points, deformation is non-homogeneous at small plastic strains, but occurs in a localised fashion: Lüder bands (stretcher strains type A) are observed. These bands are undesirable, especially since they are clearly visible in polished and painted surfaces.

In addition, non-homogeneous plastic flow may be observed at higher degrees of deformation in the stress-strain curve (stretcher strains type B). This behaviour is caused by discontinuous hardening due to dynamic strain aging (Portevin-le-Chatelier effect) and progresses in severity with increasing degree of plastic strain..

Stretcher strains of type A can be eliminated by a thermo-mechanical treatment (e.g., prior deformation by rolling); one then obtains materials that are conditionally stretcher strain free (ssf) or show little stretcher strain effects (ffa).

In contrast, stretcher strains of type B cannot be eliminated. For this reason, AlMgMn and AlMg alloys may not be suitable for decorative or visible sheet parts, eg. outer car-body sheet metal parts.

AlMgSi and AlCuMg alloys, on the other hand, do not exhibit stretcher strains and are, therefore, suitable for parts which must conform to high surface quality standards.

Fields of Application of Aluminium Body Sheet Alloys

Figure 3701.02.02 lists the most important European, American and Japanese body sheet alloys.

The aluminium alloys are divided into a group of heat-treatable alloys (groups 3 - 5) and a group of non-heat-treatable alloys (group 2). The table lists the fields of application together with a reference to the presence and types of stretcher strains.

DIN	Designation	International	Stretcher strains	Fold type	Field of application (examples)
Group 1: aluminium, unalloyed					
Al99,5 W7		1050-0	none	NF	heat reflectors
Group 2: AlMg(Mn,Cr), non-heat-treatable					
AlMg2,5 W18		5052-0	(A),B	NF	internal body parts
AlMg3 W19		5754-0	A , B	NF	internal body parts
AlMg5Mn W27		5182-0	A , B	NF	internal body parts
AlMg5Mn		5152-ssf	B	NF	internal/ext. parts
Group 3: AlMgSi(Cu,Mn), heat-treatable					
-----		6009-T4	none	NF	internal/ext. parts
-----		6010-T4	none	TF	external body parts
AlMg0,4Si1,2		6016-T4	none	(NF)	external body parts
-----		6111-T4	none	TF	external body parts
Group 4: AlCuMg(Si), heat-treatable					
-----		2002-T4	none	TF	external body parts
-----		2008-T4	none	TF	external body parts
-----		2036-T4	none	TF	external body parts
-----		2038-T4	none	---	external body parts
Group 5: AlMgCu(Zn), heat-treatable (conditionally)					
-----		GZ45/30-30	(B)	NF	internal/ext. parts
-----		KS5030	(B)	NF	internal/ext. parts
Information in parenthesis () based on assumptions A, B = Stretcher strain types; ssf = no stretcher strains (type A) NF = normal fold; TF = double fold					
Source: F. Ostermann					
		Fields of Application of Aluminium Body Sheet Alloys			3701.02.02

Compositions and Properties of Aluminium Car Body Sheet Alloys

The chemical composition and the mechanical and technological properties of aluminium sheet alloys usually used in the automotive industry are tabulated in **Figure 3701.02.03** and **Figure 3701.02.04**.

3701.03 Technological Testing Methods

Whereas the tensile test and the measured tensile properties of sheet metals are significant for the characterisation of the material's quality, there are no simple relationships between the tensile properties and the forming behavior in the press. The state of stress, the strain path history, the geometrical dimensions and the tribological

conditions exert important influences during press forming, which are not duplicated by the tension test.

Designation		Composition in wt.-%					
DIN 1725	International	Si	Cu	Mn	Mg	Cr	Zn
Group 1: aluminium, unalloyed							
Al99,5	1050	----	Al ≥ 99.5%			----	
Group 2: AlMg(Mn,Cr), non-heat-treatable							
AlMg2,5	5052	----	----	----	2,5	0,2	----
AlMg3	5754	----	----	0,2	3,0	0,1	----
AlMg5Mn	5182	----	----	0,4	4,5	----	----
Group 3: AlMgSi(Cu,Mn), heat-treatable							
-----	6009	0,8	0,4	0,5	0,6	----	----
-----	6010	1,0	0,4	0,5	0,8	----	----
(AlMg0,4Si1,2)	6016	1,2	----	----	0,4	----	----
-----	6111	0,9	0,7	0,2	0,7	----	----
Group 4: AlCuMg(Si), heat-treatable							
-----	2002	0,6	2,0	----	0,8	----	----
-----	2008	0,7	0,9	----	0,4	----	----
-----	2036	----	2,6	0,3	0,5	----	----
-----	2038	0,8	1,3	0,3	0,7	----	----
Group 5: AlMgCu(Zn), heat-treatable							
-----	GZ45/30-30	----	0,4	----	4,5	----	1,5
-----	KS5030	----	0,4	----	4,5	----	----

Designation in parenthesis () = not standardised in DIN 1725

Source: F. Ostermann

 Training in Aluminium Application Technologies	Chemical Compositions of Aluminium Body Sheet Alloys	3701.02.03
---	---	------------

Designation			R _m	R _{p0,2}	A ₅	A _{gl}	n	r	I _E	β _{0max}
DIN	International	State	[N/mm ²]	[N/mm ²]	[%]	[%]	[-]	[-]	[mm]	
Group 1: aluminium, unalloyed										
Al99,5 W7	1050-0	annealed	80	40	40	28	0,25	0,85	10,5	2,1
Group 2: AlMg(Mn,Cr), non-heat-treatable										
AlMg2,5 W18	5052-0	annealed	190	90	28	24	0,30	0,68	-----	2,1
AlMg3 W19	5754-0	annealed	210	100	28	19	0,30	0,75	9,4	2,1
AlMg5Mn W27	5182-0	annealed	280	140	30	23	0,31	0,75	10,0	2,1
AlMg5Mn	5182-ssf	annealed	270	125	24	----	0,31	0,67	----	----
Group 3: AlMgSi(Cu,Mn), heat-treatable										
-----	6009-T4	na	230	125	27	----	0,23	0,70	----	----
-----	6010-T4	na	290	170	24	----	0,22	0,70	----	----
(AlMg0,4Si1,2)	6016-T4	na	240	120	28	----	0,27	0,65	10,2	2,1
-----	6111-T4	na	275	160	28	----	0,26	0,56	----	----
Group 4: AlCuMg(Si), heat-treatable										
-----	2002-T4	na	330	180	26	----	0,25	0,63	9,6	----
-----	2008-T4	na	250	140	28	----	0,28	0,58	----	----
-----	2036-T4	na	340	190	24	----	0,23	0,70	----	----
-----	2038-T4	na	320	170	25	----	0,26	0,70	----	----
Group 5: AlMgCu(Zn), heat-treatable (?)										
-----	GZ45/30-30	na	300	155	30	----	0,29	0,68	9,8	----
-----	KS5030-T4	na	275	135	30	28	0,30	0,65	9,8	2,08

na = naturally aged
I_E = Erichsen dome height for 1 mm sheet thickness

Source: F. Ostermann

 Training in Aluminium Application Technologies	Mechanical and Technological Properties of Aluminium Body Sheet Alloys	3701.02.04
---	---	------------

Technological testing methods are used to duplicate or simulate the behavior of the material in simple forming processes. During stretch forming, deformation occurs under the action of a biaxial tensile stress, at the cost of sheet thickness. During deep drawing, the sheet material flows under a radially acting tensile stress and a tangentially acting compressive stress between the drawing die and blank holder over the drawing ring radius. Depending on the close relationship of technological test with the actual drawing operation, these tests can give useful informations about the forming behaviour of the sheet material.

In most cases however, a sheet metal part is formed under the combined actions of stretch forming and deep drawing. For this reason it is difficult to make generally valid statements on the applicability of test results obtained from simple, technological testing methods.

Hydraulic Bulge Test

A hydraulic bulge test assembly is shown in **Figure 3701.03.01**. The hydraulic bulge test simulates the stretch forming process. It can also be utilised for the determination of flow curves. For this test, a circular sheet blank is firmly clamped along its circumference and then subjected to a hydraulic pressure from one side. The sheet stretches without any friction under a biaxial state of stress. Since the clamping does not allow any in-flow of metal from the flanges, stretching leads to a reduction of the sheet thickness.

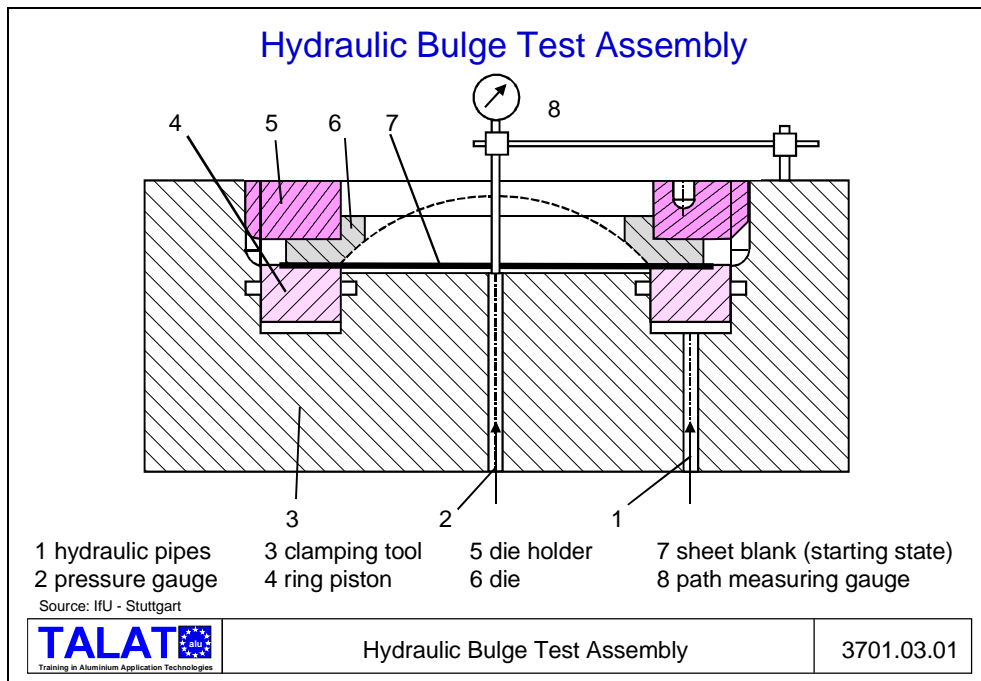


Figure 3701.03.02 summarizes the equations used to evaluate the hydraulic bulge test. For constructing the flow curve (according to Panknin), at least three values must be

determined at every step: the hydraulic pressure " p ", the radius of curvature of the spherical calotte " r " and the sheet thickness " s " at the dome.

Hydraulic Bulge Test (Formulae)				
Flow Stress	$k_f = \frac{p}{2} \left(\frac{r}{s} + 1 \right)$			
Logarithmic principal strain (principal true strain)	$\varphi = \ln \frac{s_0}{s}$			
Radius of curvature	$r = \frac{t}{2} + \frac{d_B^2}{8t}$			
<table border="1" style="width: 100%; border-collapse: collapse;"> <tr> <td style="width: 30%; text-align: center;"></td> <td style="width: 40%; text-align: center;">Hydraulic Bulge Test (Formulae)</td> <td style="width: 30%; text-align: center;">3701.03.02</td> </tr> </table>			Hydraulic Bulge Test (Formulae)	3701.03.02
	Hydraulic Bulge Test (Formulae)	3701.03.02		

Using the equation according to Panknin, it is then possible to calculate the flow stress and the deformation strain:

$$k_f = p/2 (r/s + 1)$$

$$\varphi = \ln (s_0/s)$$

When the ratio of bulge diameter to sheet thickness is large ($d_B/s_0 > 100$), a uniform radius of curvature is formed. This can be calculated from the bulge diameter d_B and the bulge depth t as follows:

$$r = t/2 + d_B^2/8t$$

Since the die has a radius of r_M , the drawn sheet has another radius of curvature r^* than that obtained by using a sharp-edged die. The Institute for Forming Technology of the University of Stuttgart used the following formula for calculating this radius:

$$r^* = t/2 + d_B^2/8t + (d_B r_M + r_M^2)/2t - r_M$$

The above formula delivers the same results for the radius of curvature that Panknin obtains with his formula for the correction of the measured bulge depth and using this correction for calculating the actual bulge diameter.

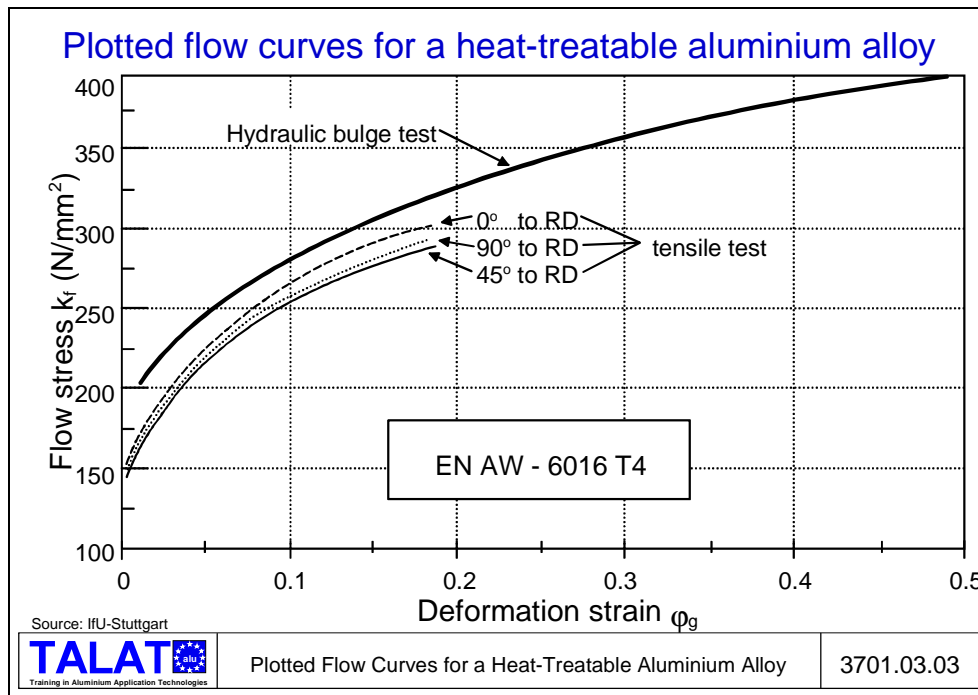
When the ratio bulge diameter/sheet thickness ($d_B/s_0 > 100$) is large, the transverse stress can be neglected. In this case, the flow stress can be calculated using the formula:

$$k_f = pr/2s$$

For calculating the radius of bulge curvature r , the die radius r_M can be taken into account. The corrected radius of curvature r^* can then be substituted in the above formula for the calculation of the flow stress.

Plotted Flow Curves for a Heat-Treatable Aluminium Alloy

The curves plotted in **Figure 3701.03.03** are obtained by evaluating the results of a test series. Curves for the hydraulic bulge test (calculated using the corrected radius of curvature r^*) as well as the flow curves determined using flat tensile specimens (0° , 45° and 90° to rolling direction) have been depicted.



The flow curve obtained from the hydraulic bulge test lies higher than those for the flat tensile specimens. This deviation is due partly to the biaxial state of stress as well as due to the anisotropy. The plots show very clearly that much higher deformation strains can be obtained using the hydraulic bulge test than with the flat tensile specimen.

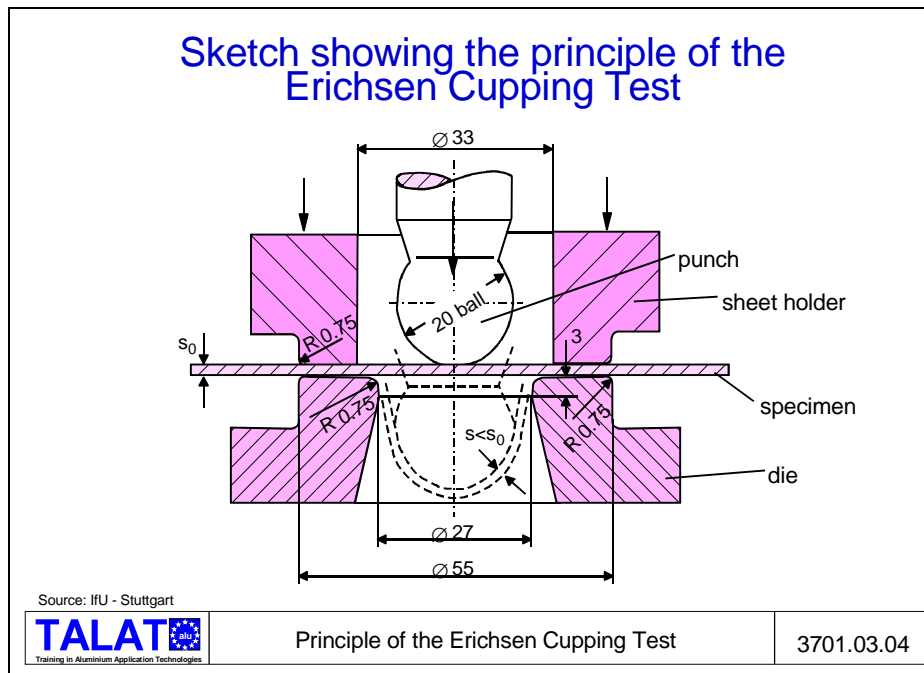
The grain size affects the sheet surface obtained after forming. This effect can be clearly seen in forming tests without tool contact (e.g. hydraulic bulge test or Erichsen cupping test). The larger the grain size, the rougher is the sheet surface obtained. This is also referred to as "orange peeling".

Erichsen Cupping Test

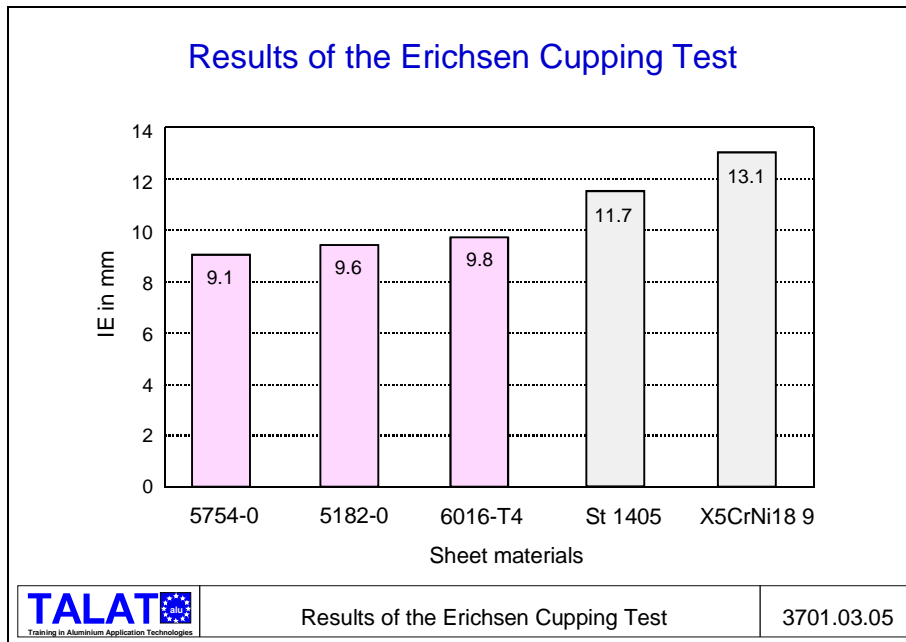
The Erichsen cupping test is used to assess the stretch formability of sheets. This test can be classified as a stretch forming test which simulates plane stress biaxial tensile deformation.

For the Erichsen test a sheet specimen blank is clamped firmly between blankholders which prevents the in-flow (feeding) of sheet volume from under the blankholder into the deformation zone during the test. The standardised dimensions of the test set-up are shown in **Figure 3701.03.04**. The ball punch is forced onto the sheet specimen till

cracks begin to appear in the bulge dome. The distance the punch travels is referred to as the Erichsen drawing index IE (index Erichsen) and is a measure for the formability of the sheet during stretch forming.



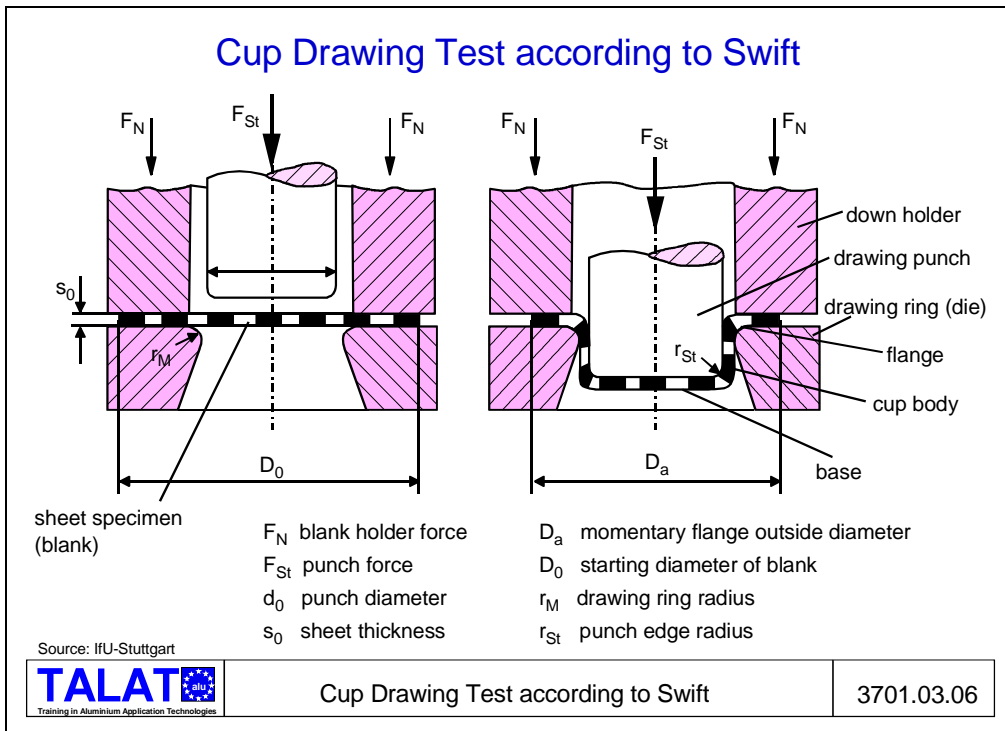
The cupping test according to Erichsen is standardised in DIN 50 101, part 1 and carried out using, for example, an Erichsen universal cupping test machine, model 142/20 of the Erichsen company. Rectangular sheet specimens are cut out and clamped without any lubrication between two ring dies. A ball punch (diameter = 20 mm) is forced into the sheet until fracture occurs. The distance the punch moves before cracks begin to appear (height of dome) is measured. The test results (average values for 3 tests) are depicted in **Figure 3701.03.05** for different aluminium alloys and, for purposes of comparison, for some steels.



The stretch formability as measured by the Erichsen test depends on sheet thickness s . The formability index increases with increasing sheet thickness. A comparison of formability by Erichsen relies therefore on results obtained with the same sheet thickness.

Cup Drawing Test according to Swift

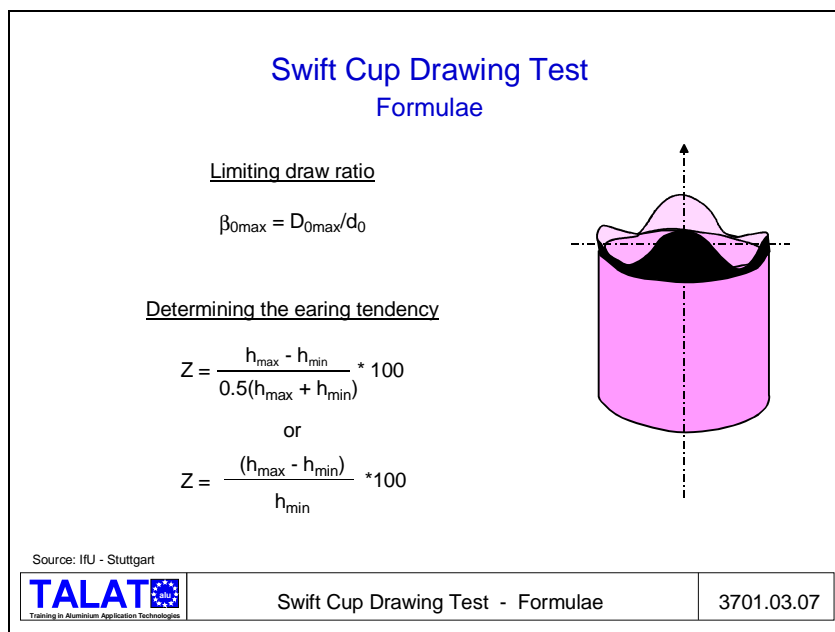
Another method for determining the formability of a sheet is by using the cup deep drawing test according to Swift, s. **Figure 3701.03.06**. This test is conducted using a flat punch and simulates pure deep drawing characterized primarily by a plane tension-compression state of stress under the blank holder. This test is not standardised, although the international deep drawing group (IDDRG) has issued a guideline for it.



A series of circular blanks with a gradually increasing diameter D_0 is drawn to cylindrical cups using a punch with constant diameter d_0 , till a limiting value is reached, just before the first base cracks begin to appear. The maximum blank diameter D_{0max} thus determined, is taken as a measure for deep drawability, see **Figure 3701.03.07**. The limiting draw ratio is given by the ratio:

$$\beta_{0max} = D_{0max}/d_0$$

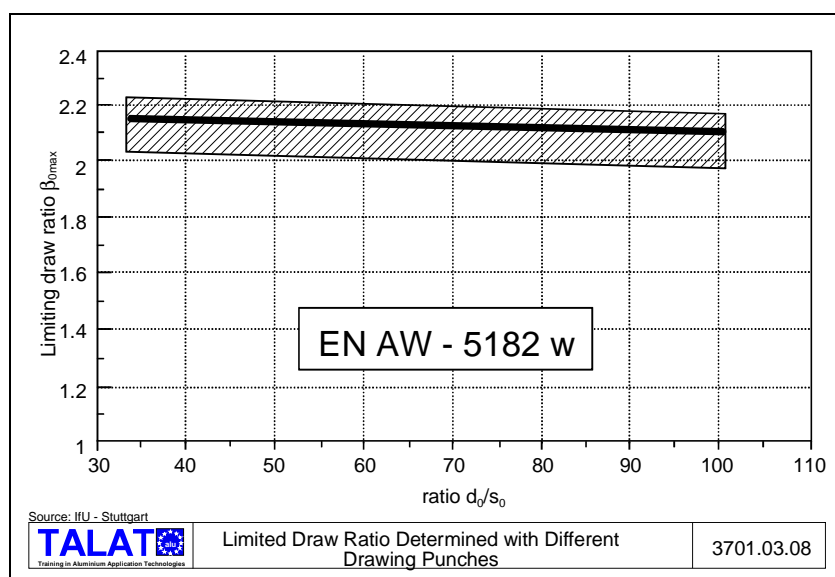
The cup deep drawing test according to Swift can also be utilised to determine the earing tendency. The phenomenon of earing is a result of the directionality of the plastic properties of the material (anisotropy). The earing tendency Z is measured using drawn cups with flat bases. The heights, measured from the cup base to the ear peak and the ear valley respectively, are referred to h_{max} and h_{min} .



The two formulae shown in **Figure 3701.03.07** for the calculation of the earing tendency Z give slightly different results. A low value of Z is indicative of a low tendency to earing.

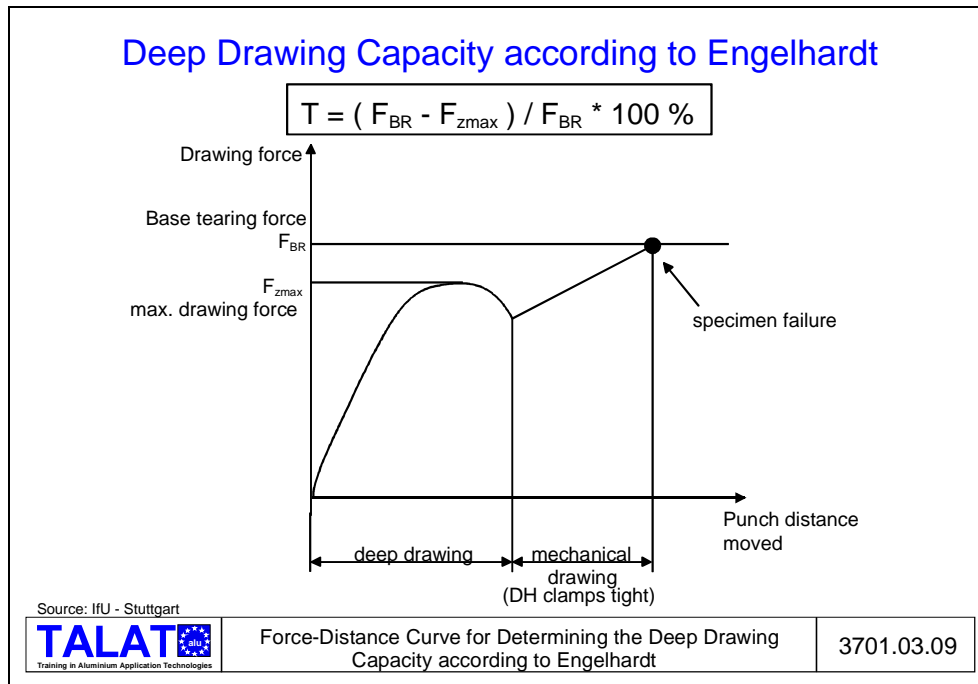
Effect of the Blank Diameter to Thickness Ratio on Limiting Draw Ratio

The results of tests conducted with a non-heat-treatable aluminium alloy (EN-AW 5182-0) are shown in **Figure 3701.03.08**. For this test series, punches with different diameters were used. It was found that the limiting draw ratio depends on friction (lubrication) of the flange under the blank holder. This influence is larger for punches with larger diameters (flange area is larger). Therefore, β_{0max} is not only a function of material but also a function of the lubricant and the sheet surface structure.



Drawability of Materials according to Engelhardt

The deep drawing and rupture test method according to Engelhardt is a combination of test methods for formability of sheets and a simplification of the deep drawing cupping test. The disadvantage of the deep drawing cupping test is due to the fact that a large number of tests are needed to be able to determine the limiting draw ratio with sufficient accuracy. In contrast, the testing of sheets according to Engelhardt requires only a single specimen.

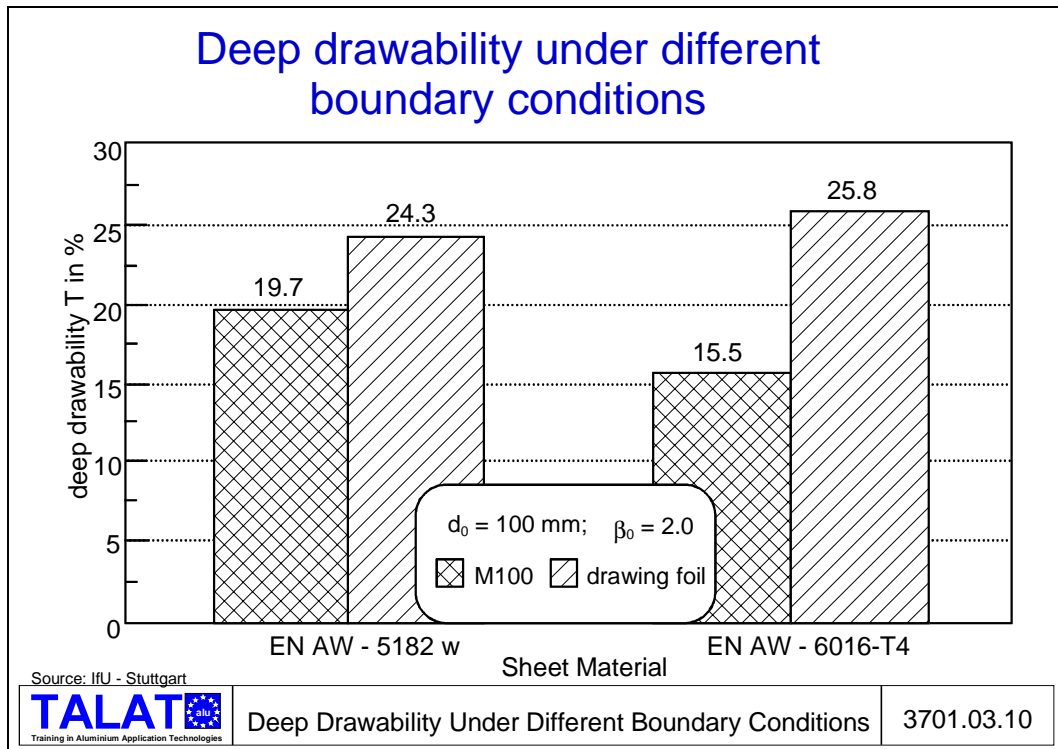


A flat punch is forced into a blank made of the test material until a drawing force maximum F_{zmax} is exceeded, see **Figure 3701.03.09**. Then the remaining cup flange is arrested under the blankholder and the punch forced further into the cup till fracture occurs in the bottom. The drawing force F_z and F_{zmax} , respectively, and the bottom break force F_{BR} are measured. Now it is possible to determine a characteristic value T , which gives the measure of the drawability, i.e., the safety with which a certain cup type can be formed without cracks and fracture appearing in the cup base:

$$T = (1 - F_{zmax}/F_{BR}) * 100 \%$$

Under constant testing conditions, the drawability is also a material characteristic.

Figure 3701.03.10 shows the results obtained using aluminium sheet specimens made of the non-heat-treatable alloy AlMg5Mn-w (EN-AW 5182-0) and the heat-treatable alloy AlMg0,4Si1,2 ka (EN-AW 6016-T4). The (Engelhardt) drawability was measured using a tool with a punch diameter $d_0 = 100 \text{ mm}$ and $\beta_0 = 2.0$ ($D_0 = 200 \text{ mm}$). **Figure 3701.03.10** illustrates that the drawing capacity reserve also depends on the frictional conditions. Drawing with a lubricant foil gives other (higher) values than obtained with mineral oil lubricants.



Creating the Forming Limit Diagram (FLD)

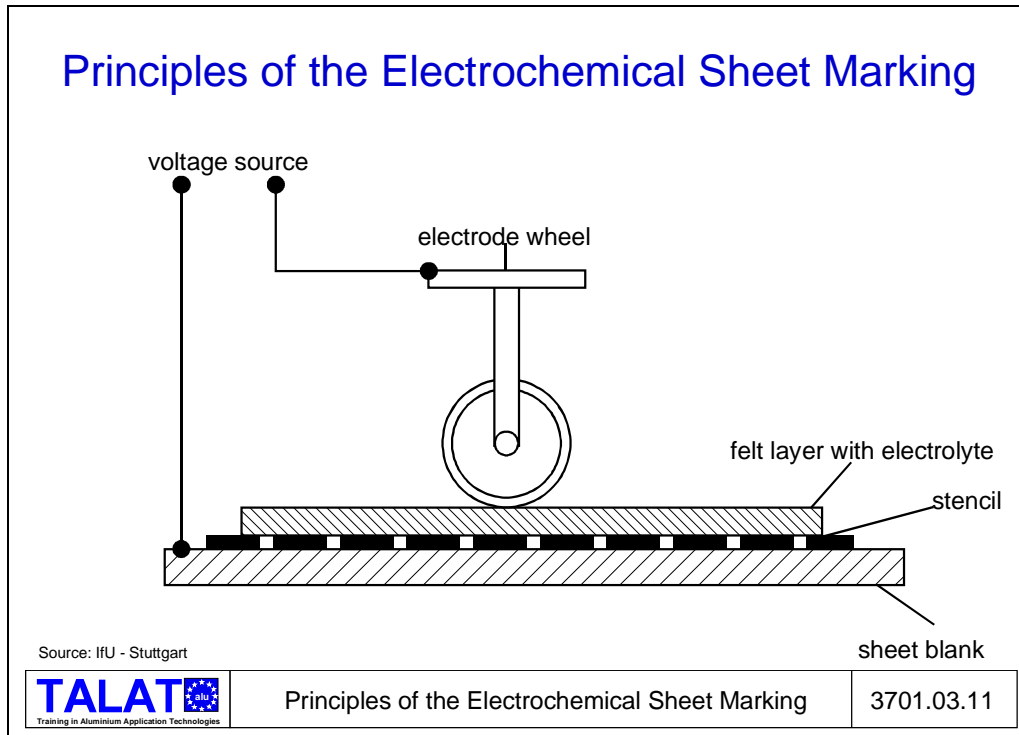
With the help of Forming Limit Diagrams it is possible to determine the limiting deformations, e.g. necking and tearing, which eventually lead to failure. This chart utilises the line grid deformation analysis to measure the forming properties of sheets. The line grid deformation analysis is based on the assumption that sheet materials fail due to necking or rupture which is a result only of a plane state of stress being reflected in a local measurable deformation. In order to be able to determine the local deformation of the formed sheet, line patterns with defined geometries (e.g. circles, grids) are marked on the sheet specimens prior to forming. The subsequent forming process causes the line patterns to deform by an amount which depends on the local deformation experienced by the sheet part. The distortions in the line patterns are measured and evaluated to deliver information about the local deformation in widths.

The deformation in thickness can be derived using the law of volume constancy and the resulting correlation:

$$\varphi_1 + \varphi_2 + \varphi_3 = 0$$

A number of methods are available for marking line patterns on sheet specimens, some of which are engraving, printing (silk-screen process, offset printing), photochemical or electrochemical marking. While choosing the appropriate process, care should be taken that the chosen process does not influence the forming, which e.g., would be the case in too deeply engraved patterns with accompanying notch effects. The pattern must also be able to resist the influences of the forming process, like friction or lubricants. Further, it should be possible to apply the marking with as little effort as possible. The electrochemical method is very often chosen. In this method, a textile stencil, in which

only the circular ring areas allow the etching agent to pass through, is laid out on the surface of the sheet, see **Figure 3701.03.11**. A substance soaked lightly with etching agent is then laid on this stencil. Under the pressure of the rolling wheel, the chemicals are pressed out through the contours of the stencil and reach the surface of the sheet. As a result of the voltage laid across the wheel and the conducting sheet, the etchant is activated, etching the circular ring pattern of the stencil on to the sheet surface.



Patterns of different geometrical shapes and sizes can thus be etched on the sheet (lines, circles, separate or overlapping).

The distortion of the circles alone does not indicate how much the sheet metal can still be deformed before failure through necking or tearing will occur. For this reason, laboratory tests are conducted with the same material to obtain Forming Limit Diagrams. The results of the deformation analysis on the production part are then compared with the FLD. Thus, one obtains an indication about how "far away" the material still is from failure, e.g. if the material has almost reached the limits of its formability or whether its quality may be "too good" for the real component.

In order to create a FLD, sheet specimens of different sizes and shapes are used so that it is possible to obtain different states of deformation. Thus, one uses circular blanks as well as semi-circular blanks with side cuts of different radii, see **Figure 3701.03.12**.

A circular grid pattern is marked on the specimen blanks which are subsequently clamped firmly in the test rig and drawn with a spherical punch till tearing occurs. After removal from the rig the distorted circles of the grid are evaluated.

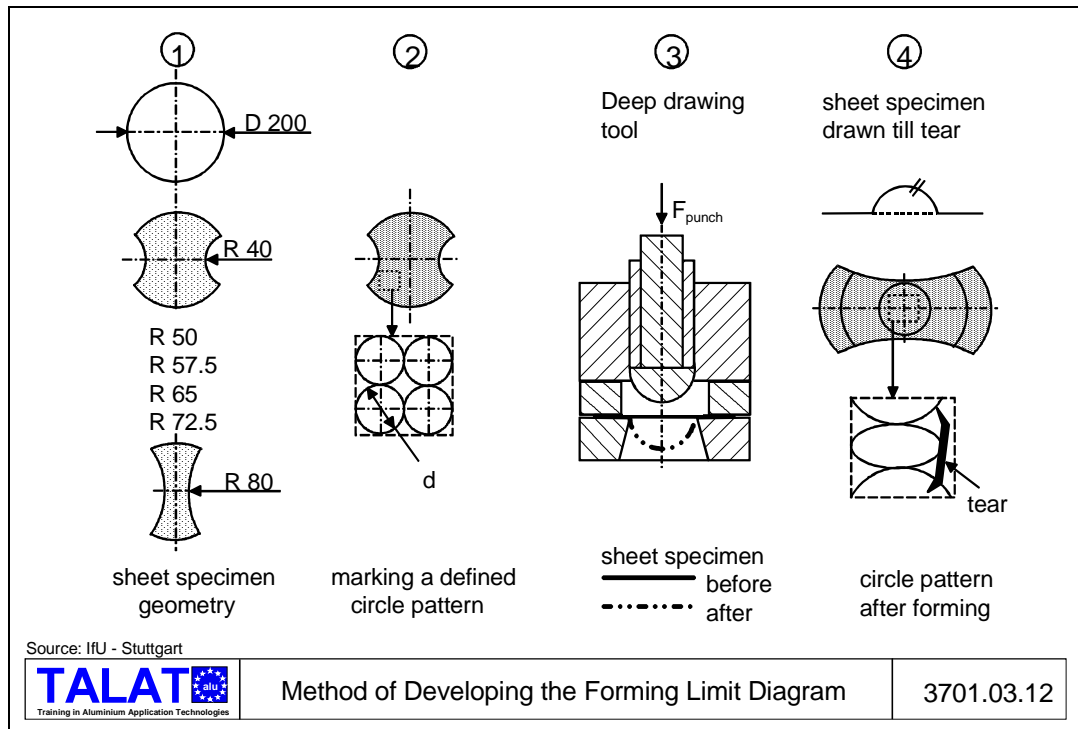
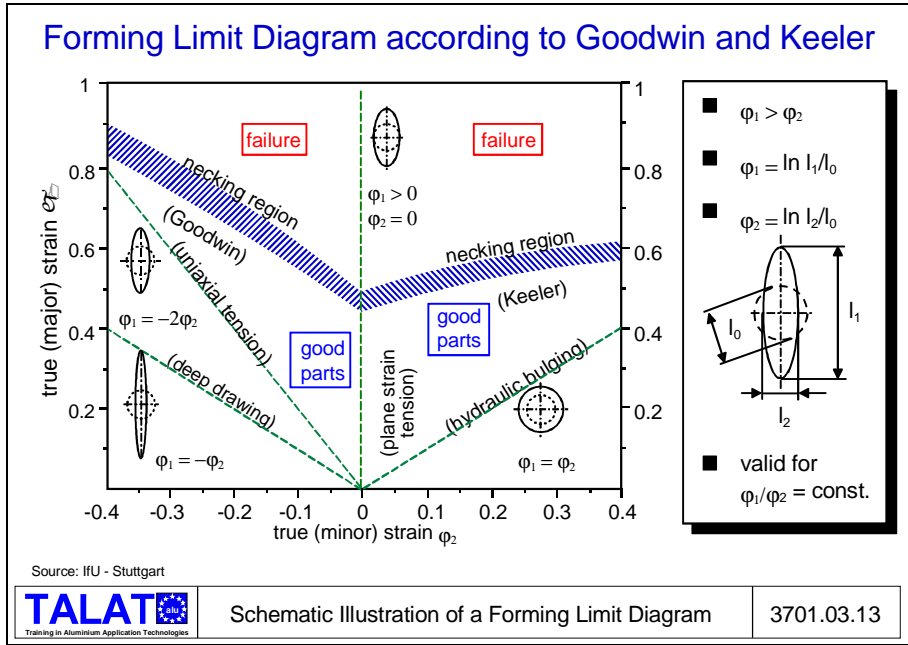


Figure 3701.03.13 depicts the changes in the circular grid dimensions which occur under the different stressing conditions used to create the FLD. The left-hand-side of the diagram shows distortions which occur when the sheet is subjected to pure drawing ($\varphi_1 = -\varphi_2$) up to the distortions which occur during the hydraulic bulge test ($\varphi_1 = \varphi_2$). The deformation $\varphi_1 = -2\varphi_2$, is valid for the uniaxial tensile test. On the right-hand-side, the deformation $\varphi_2 = 0$ results when the transverse contraction is hindered, e.g., bending of wide sheets. The condition $\varphi_2 = 0$ is also called plane strain forming. It can be clearly seen that, depending on the state of stress, the circles (shown as dotted lines) are distorted into different elliptical shapes. The degrees of deformation φ_1 and φ_2 , can be calculated from the starting diameter of the circle d , and the longer (l_1) and shorter (l_2) axes of the ellipse. The valid condition is $\varphi_1 \geq \varphi_2$. The deformation strain φ_3 (in the direction of the sheet thickness) can be calculated from the condition of continuity (volume constancy):

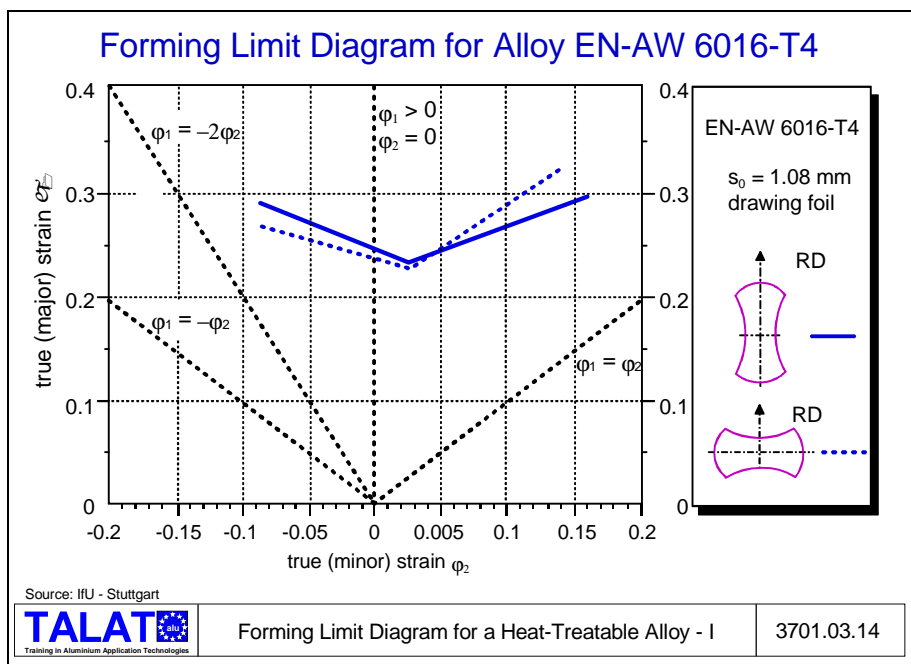
$$\varphi_3 = -\varphi_1 - \varphi_2$$

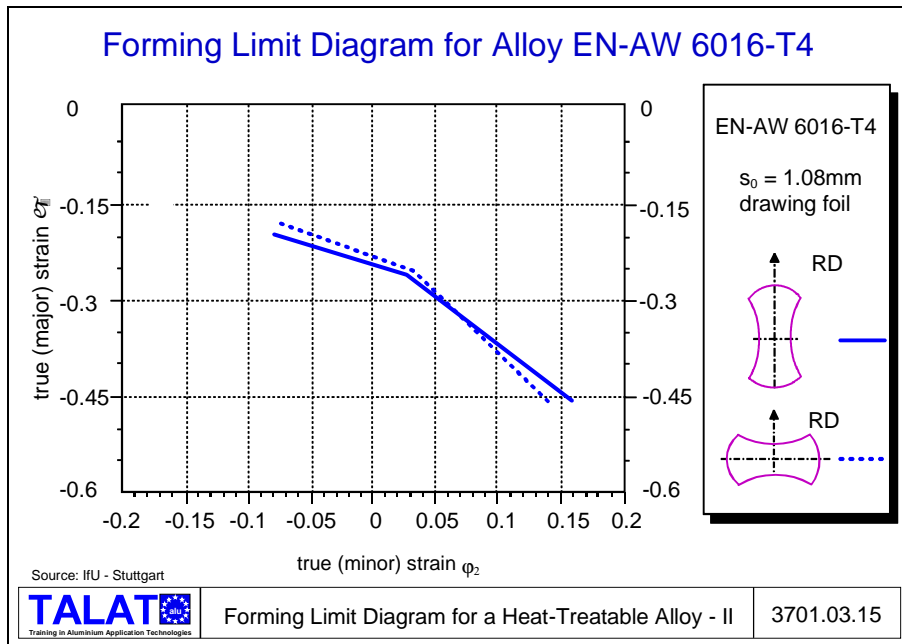
The tests described here were conducted with a hemispherical punch having a diameter of 100 mm. The sheet specimens had side cuts of different radii and were mechanically drawn till tearing occurred. The side cuts (on the specimen sheets) of different depths and radii cause strain deformations φ_1 and φ_2 of different values on the sheets. A total of seven different sheet specimen forms were used. All sheet specimens were electrochemically marked with a an Erichsen sheet marking apparatus and a stencil to deliver a pattern of circles, each 8 mm in diameter.



After drawing, the circles in the immediate vicinity of the tear were measured in the direction of maximum elongation and transverse to it. In order to prevent faulty interpretations due to tearing and associated dilation of the ellipses, only complete ellipses and circles were evaluated.

Figure 3701.03.14 and **Figure 3701.03.15** are examples of Forming Limit Diagrams for sheet alloy EN-AW 6016-T4. They show the FLD for forming limits measured in the sheet plane (ϕ_1/ϕ_2) and calculated for the through-thickness plane (ϕ_2/ϕ_3), respectively. The sheet specimen used was covered with a foil and additionally lubricated with lubricant oil M100 on the punch side, in order to minimize the influence of friction on the results as much as possible.





The charts clearly show the slight differences in the forming limits with respect to the rolling direction and transverse direction.

The diagrams shown are valid for a constant ratio of ϕ_1/ϕ_2 . Deviations from this proportional strain path will greatly affect the position of the forming limit curve. This fact limits the usefulness of the FLD for determination of forming limits for actual parts with complex shapes. The main advantage of the FLD in sheet metal drawing is to point the way to solutions in the design of forming tools with respect to achieving optimum flow of the sheet metal in the die.

3701.04 List of Figures

Figure No.	Figure Title (Overhead)
3701.01.01	Stress-Strain Diagram and Flow Curves
3701.01.02	Preparing Tensile Test Specimen from a Sheet
3701.01.03	Stress-Strain Diagram for a Heat-Treatable Alloy
3701.01.04	Stress-Strain Diagram for a Non-Heat-Treatable Alloy
3701.01.05	Flow Curves of a Heat-Treatable Alloy
3701.01.06	Flow Curves of a Non-Heat-Treatable Alloy
3701.01.07	Definition of the Strain-Hardening Exponent n
3701.01.08	Schematic Illustration of a Flat Tensile Specimen
3701.01.09	Definition of Anisotropy Values
3701.01.10	Anisotropy as a Function of the Rolling Direction
3701.01.11	Representation of the Vertical Anisotropy Using Polar Coordinates
3701.02.01	Materials with and without Stretcher Strains
3701.02.02	Fields of Application of Aluminium Body Sheet Alloys
3701.02.03	Chemical Compositions of Aluminium Body Sheet Alloys
3701.02.04	Mechanical and Technological Properties of Aluminium Body Sheet Alloys
3701.03.01	Hydraulic Bulge Test Assembly
3701.03.02	Hydraulic Bulge Test (Formulae)
3701.03.03	Plotted Flow Curves for a Heat-Treatable Aluminium Alloy
3701.03.04	Principle of the Erichsen Cupping Test
3701.03.05	Results of the Erichsen Cupping Test
3701.03.06	Cup Drawing Test according to Swift
3701.03.07	Swift Cup Drawing Test - Formulae
3701.03.08	Limiting Draw Ratio Determined with Different Drawing Punches
3701.03.09	Force-Distance Curve for Determining the Deep Drawing Capacity according to Engelhardt
3701.03.10	Deep Drawability under Different Boundary Conditions
3701.03.11	Principles of the Electrochemical Sheet Marking
3701.03.12	Method of Developing the Forming Limit Diagram
3701.03.13	Schematic Illustration of a Forming Limit Diagram
3701.03.14	Forming Limit Diagram for a Heat-Treatable Alloy - I
3701.03.15	Forming Limit Diagram for a Heat-Treatable Alloy - II